

Tailoring the gas separation efficiency of Metal Organic Framework ZIF-8 through metal substitution: a computational study

Panagiotis Krokidas¹, Salvador Moncho², Edward N. Brothers², Marcelo Castier¹
and Ioannis G. Economou^{1,*}

¹Chemical Engineering Program, Texas A&M University at Qatar, P.O. Box 23874, Education City, Doha, Qatar

²Science Program, Texas A&M University at Qatar, P.O. Box 23874, Education City, Doha, Qatar

*Corresponding author at ioannis.economou@qatar.tamu.edu

The force field terms are presented from the most flexible framework (CdIF-1) to the stiffest (BeIF-1), so the reader can follow the decrease in all bond lengths and the increase in angle constants, where the metal ion is involved. Parameter values for the Lennard-Jones (LJ) potential are based on the AMBER force field¹ and can be found in the work of Hertag et al.² The atom types are shown in Figure S3, at the end of the document.

Table S1. CdIF-1 framework bond stretching and bond angle bending parameters.

Bond	l_0 (Å)	k_l (kJ/mol/nm ²)	Angle	θ_0 (degrees)	k_θ (kJ/mol/rad ²)
Cd-N	2.257	45354.6	N-Cd-N	109.5	205.85
N-C2	1.357	265767.7	Cd-N-C2	130.2	356.48
N-C1	1.373	267608.6	Cd-N-C1	125.1	364.85
C1-C1	1.375	343004.3	C1-N-C2	104.6	1026.75
C1-H1	1.078	325598.9	C1-C1-N	107.6	900.40
C2-C3	1.497	205267.0	C1-C1-H1	130.6	551.45
C3-H2	1.092	284177.3	C2-C3-H2	110.9	564.00
			H2-C3-H2	108.0	317.98
			N-C2-N	113.9	936.38
			N-C2-C3	122.9	942.24
			N-C1-H1	121.6	547.27

Table S2. ZIF-8 framework bond stretching and bond angle bending parameters.

Bond	l_0 (Å)	k_l (kJ/mol/nm ²)	Angle	θ_0 (degrees)	k_θ (kJ/mol/rad ²)
Zn-N	2.048	52802.1	N-Zn-N	109.5	296.23
N-C2	1.360	257818.1	Zn-N-C2	130.3	462.75
N-C1	1.376	253048.3	Zn-N-C1	125.1	475.30
C1-C1	1.375	339991.8	C1-N-C2	104.5	1077.80
C1-H1	1.077	327690.9	C1-C1-N	107.9	909.61
C2-C3	1.498	203760.8	C1-C1-H1	130.6	552.29
C3-H2	1.091	286855.0	C2-C3-H2	110.8	565.68
			H2-C3-H2	108.1	317.98
			N-C2-N	113.8	955.63
			N-C2-C3	123.1	958.97
			N-C1-H1	121.5	549.78

Table S3. ZIF-67 framework bond stretching and bond angle bending parameters.

Bond	l_0 (Å)	k_l (kJ/mol/nm ²)	Angle	θ_0 (degrees)	k_θ (kJ/mol/rad ²)
Co-N	2.044	58910.7	N-Co-N	109.5	924.66
N-C2	1.361	253383.0	Co-N-C2	130.8	534.72
N-C1	1.377	249952.2	Co-N-C1	124.7	537.23
C1-C1	1.375	340242.9	C1-N-C2	104.4	1074.45
C1-H1	1.077	327774.6	C1-C1-N	107.9	920.48
C2-C3	1.498	286101.9	C1-C1-H1	130.6	551.45
C3-H2	1.091	286101.0	C2-C3-H2	110.8	564.84
			H2-C3-H2	108.1	317.98
			N-C2-N	113.9	964.83
			N-C2-C3	123.1	974.87
			N-C1-H1	121.5	550.61

Table S4. BeIF-1 framework bond stretching and bond angle bending parameters.

Bond	l_0 (Å)	k_l (kJ/mol/nm ²)	Angle	θ_0 (degrees)	k_θ (kJ/mol/rad ²)
Be-N	1.749	56400.3	N-Be-N	109.5	550.61
N-C2	1.364	254219.840	Be-N-C2	130.1	671.95
N-C1	1.376	262253.1	Be-N-C1	125.6	686.18
C1-C1	1.375	342753.3	C1-N-C2	104.4	1128.84
C1-H1	1.077	320201.3	C1-C1-N	108.1	941.40
C2-C3	1.498	203091.4	C1-C1-H1	128.6	533.04
C3-H2	1.091	286937.7	C2-C3-H2	110.8	557.31
			H2-C3-H2	108.1	317.98
			N-C2-N	113.8	1028.43
			N-C2-C3	123.9	1006.67
			N-C1-H1	121.4	558.98

Table S5. Torsional potential parameters (common for all frameworks).

Dihedral	φ_0 (degrees)	m	k_φ (kJ/mol)	Source
N-C1-C1-N	180	2	90.0	AMBER
N-C1-C1-H1	180	2	90.0	AMBER
C1-C1-N-M	180	2	25.1	AMBER
C1-C1-N-C2	180	2	25.1	AMBER
C3-C2-N-M	180	2	41.8	AMBER
C3-C2-N-C1	180	2	41.8	AMBER

Table S6. Partial charges.

Atom type	Partial charge (e)			
	CdIF-1	ZIF-8	ZIF-67	BeIF-1
M	1.1901	1.3429	1.3497	1.6627
N	-0.6532	-0.6822	-0.6956	-0.6646
C1	-0.0583	-0.0622	-0.0581	-0.0896
C2	0.7379	0.7551	0.7846	0.6287
H1	0.095	0.0912	0.0910	0.0875
C3	-0.2771	-0.2697	-0.3094	-0.1824
H2	0.059	0.0499	0.0584	0.0186

Table S7. Experimental and calculated from MD simulations representative structural values (bond lengths, bond angles and metal-metal distance) of the ZIF variations.

BeIF-1 (Be)		ZIF-67 (Co)		ZIF-8 (Zn – original)		CdIF-1 (Cd)	
Expt.	MD	Expt. [3]	MD	Expt. [4]	MD	Expt. [5]	MD
Bond length							
(Å)							
M-N	N/A	1.73	1.95	1.96	1.99	1.98	2.20
C2-N	N/A	1.36	1.38	1.34	1.34	1.35	N/A
C1-N	N/A	1.38	1.38	1.39	1.37	1.38	N/A
C1-C1	N/A	1.37	1.37	1.38	1.35	1.37	N/A
C2-C3	N/A	1.50	1.49	1.49	1.49	1.49	N/A
M-M	N/A	5.54	5.98	5.99	6.00	6.00	6.39
Bond angle							
(deg)							
C1-C1-N	N/A	109.1	108.7	108.5	108.7	108.5	N/A
C1-N-M	N/A	127.9	127.0	128.3	126.4	127.0	N/A
C2-N-M	N/A	129.4	129.4	129.6	128.4	128.8	N/A
C1-N-C2	N/A	104.7	106.5	104.0	105.2	105.0	N/A
N-M-N	N/A	109.5	109.5	109.5	109.8	109.5	N/A
N-C2-N	N/A	113.0	112.0	115.6	112.2	113.4	N/A
N-C2-C3	N/A	123.4	125.0	122.2	123.9	123.2	N/A

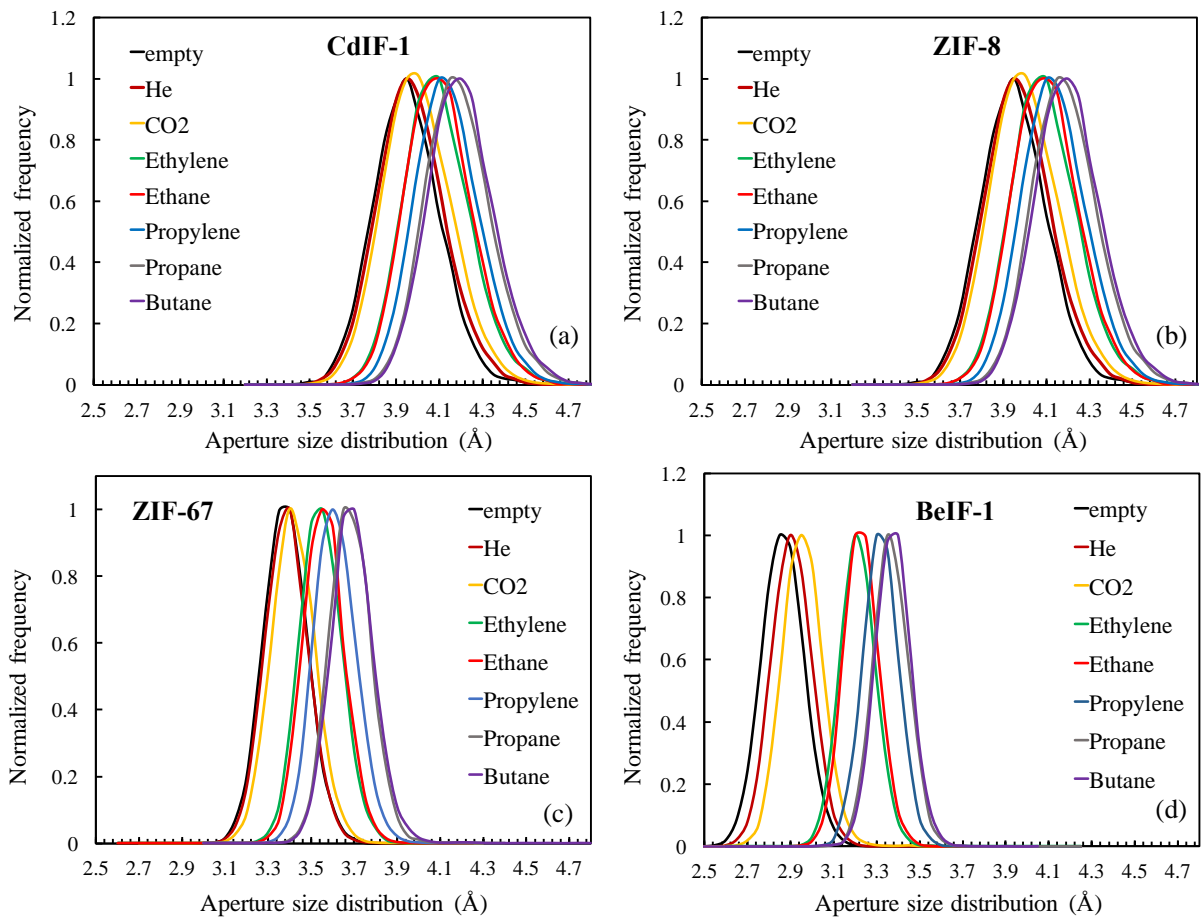


Figure S1. Aperture size distributions shifts for various gases exposure in (a) CdIF-1, (b) ZIF-8, (c) ZIF-67 and (d) BeIF-1 apertures, used to extract the mean aperture values in Table 4 and Table S8.

Table S8. Average aperture diameter for all frameworks and various penetrants.

	Mean aperture size (Å)			
	CdIF-1	ZIF-8	ZIF-67	BeIF-1
Empty	3.92	3.43	3.33	2.84
He	3.93	3.45	3.36	2.89
CO ₂	3.97	3.46	3.40	2.93
Ethylene	4.05	3.64	3.50	3.17
Ethane	4.07	3.65	3.52	3.20
Propylene	4.17	3.75	3.65	3.29
Propane	4.18	3.78	3.70	3.34
<i>n</i> -Butane	4.19	3.79	3.70	3.35

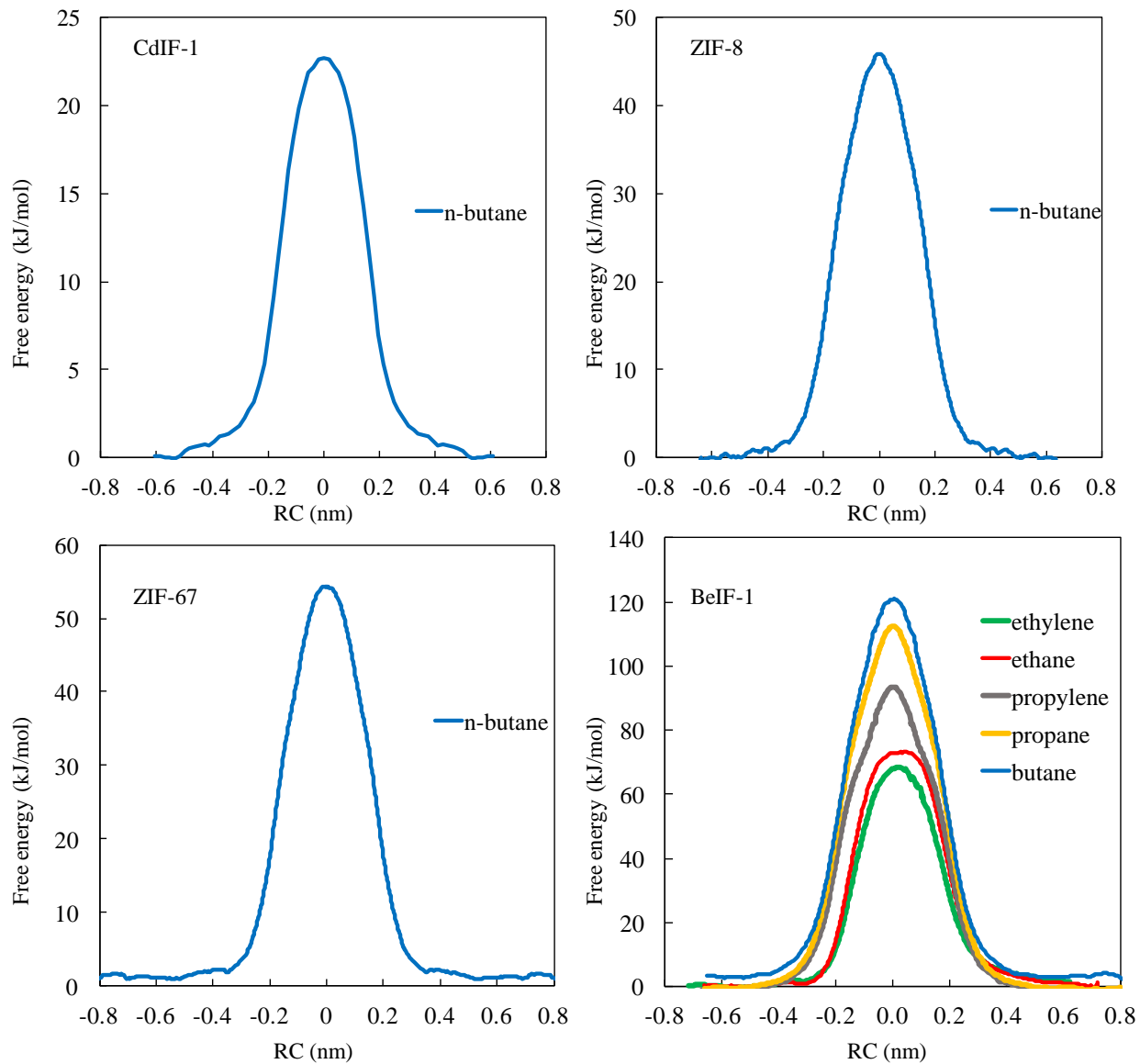


Figure S2. Free energy profiles for various gas molecules from umbrella samplings in CdIF-1, ZIF-8, ZIF-67 and BeIF-1.

The free energy profiles for each case is the outcome of multiple umbrella samplings that were processed to get an average profile. We used the Bayesian bootstrap method, with the use of g-wham software, as proposed by Hub et al,⁶ in which umbrellas are selected among the set of available ones (these consist of our repetitions of umbrella trajectories with different initial conditions, as discussed in the main text) with a random weight in order to construct a new set, that results in a new final profile. This procedure is repeated multiple times and an average profile

is extracted. More details on the bootstrap methods available in g-wham, can be found in the accompanying publication of the developers.⁶

Table S9. Cage-to-cage hoping rates ($k_{A \rightarrow B}$) and correction factors (κ) for TST calculated diffusivities of the various gas molecules in the ZIF frameworks of this work. The location of the dividing surface (distance from aperture center in Å) for each case is included for verification and reproducibility.

ZIF	molecule	Dividing surface at: (in Å)	$k_{A \rightarrow B}$	κ
ZIF-8	<i>n</i> -Butane	0.60	3.7×10^3	0.27
ZIF-67	<i>n</i> -Butane	0.6	1.2×10^2	0.20
	Ethylene	0.24	1.8×10^0	0.22
	Ethane	0.24	1.6×10^{-1}	0.26
BeIF-1	Propylene	0.20	5.5×10^{-5}	0.03
	Propane	0.20	4.8×10^{-8}	0.04
	<i>n</i> -Butane	0.60	2.0×10^{-9}	0.06

Table S10. Molecular sizes and mean aperture sizes used for the estimation of the expansion ratio of CdIF-1, ZIF-8, ZIF-67 and BeIF-1 for various molecules as plotted in Figure 9, along with corresponding diffusivities from this work and from the literature (available only for ZIF-8 and ZIF-67).^{7,8,9}

ZIF	guest molecule	Molecule Size (Å)	Mean Aperture (Å)	Expansion Ratio	Diffusivities (m ² /sec)			
					D_o [This work]	D_s TST [7]	D_o Expt. [8]	D_o Expt. [9]
CdIF-1	He	2.66	3.93	1.48	$(6.0\pm 0.5)\times 10^{-8}$			
	CO ₂	3.24	3.97	1.23	$(1.7\pm 0.3)\times 10^{-9}$			
	Ethylene	3.59	4.05	1.13	$(3.5\pm 0.9)\times 10^{-9}$			
	Ethane	3.72	4.07	1.09	$(2.0\pm 0.8)\times 10^{-9}$			
	Propane	4.16	4.18	1.00	$(6.5\pm 1.0)\times 10^{-10}$			
	<i>n</i> -Butane	4.52	4.52	0.93	$(1.0\pm 0.4)\times 10^{-11}$			
ZIF-8	He	2.66	3.45	1.30	$(5.0\pm 0.8)\times 10^{-9}$	1.61×10^{-8}	6.5×10^{-8}	
	CO ₂	3.24	3.46	1.07	$(2.9\pm 0.4)\times 10^{-10}$	4.6×10^{-10}	2.1×10^{-10}	
	Ethylene	3.59	3.64	1.01	$(6.5\pm 0.9)\times 10^{-11}$	5.7×10^{-11}	3.6×10^{-11}	
	Ethane	3.72	3.65	0.98	$(3.0\pm 0.8)\times 10^{-11}$	1.5×10^{-11}	8.8×10^{-12}	
	Propylene	4.03	3.75	0.93	$(1.8\pm 0.1)\times 10^{-12}$	2.4×10^{-12}	2.0×10^{-12}	1.3×10^{-12}
	Propane	4.16	3.78	0.91	$(4.0\pm 1.5)\times 10^{-14}$	8.2×10^{-13}	2.0×10^{-14}	3.7×10^{-14}
	<i>n</i> -Butane	4.52	3.80	0.84	$(1.0\pm 0.8)\times 10^{-15}$	9.5×10^{-15}	5.7×10^{-16}	
ZIF-67	He	2.66	3.36	1.26	$(5.0\pm 0.5)\times 10^{-9}$			
	CO ₂	3.24	3.40	1.05	$(2.2\pm 0.6)\times 10^{-10}$			
	Ethylene	3.59	3.50	0.98	$(2.0\pm 0.6)\times 10^{-11}$			
	Ethane	3.72	3.52	0.95	$(4.0\pm 0.8)\times 10^{-12}$			
	Propylene	4.03	3.65	0.91	$(3.0\pm 0.1)\times 10^{-13}$			1.5×10^{-12}
	Propane	4.16	3.70	0.88	$(1.5\pm 0.5)\times 10^{-15}$			8.0×10^{-16}

	<i>n</i> -Butane	4.52	3.70	0.81	$(5.6\pm1.3)\times10^{-17}$
BeIF-1	He	2.66	2.88	1.08	$(5.0\pm0.7)\times10^{-9}$
	CO ₂	3.24	2.93	0.90	$(4.5\pm0.5)\times10^{-12}$
	Ethylene	3.59	3.17	0.88	$(5.6\pm0.8)\times10^{-19}$
	Ethane	3.72	3.20	0.86	$(1.0\pm0.2)\times10^{-19}$
	Propylene	4.03	3.29	0.82	$(5.0\pm1.0)\times10^{-24}$
	Propane	4.16	3.34	0.80	$(3.0\pm0.3)\times10^{-27}$
	<i>n</i> -Butane	4.52	3.35	0.74	$(7.7\pm0.2)\times10^{-28}$

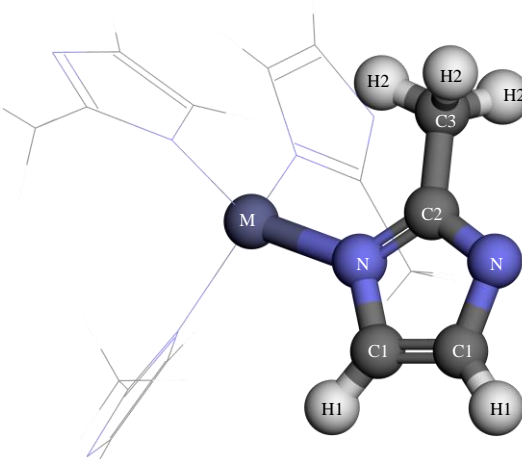


Figure S3. Highlighted 2-methylimidazole in tetrahedral unit (in bold outline) introduces the force field atom types of this work (M stands for metal: Be, Co, Zn, Cd).

- (1) Duan, Y.; Wu, C.; Chowdhury, S. S.; Lee, M. C.; Xiong, G.; Zhang, W.; Yang, R.; Cieplak, P.; Luo, R.; Lee, T.; et al. A Point-Charge Force Field for Molecular Mechanics Simulations of Proteins Based on Condensed-Phase Quantum Mechanical Calculations. *J. Comput. Chem.* **2003**, *24*, 1999–2012.
- (2) Hertag, L.; Bux, H.; Caro, J.; Chmelik, C.; Remsungnen, T.; Knauth, M.; Fritzsch, S. Diffusion of CH₄ and H₂ in ZIF-8. *J. Memb. Sci.* **2011**, *377*, 36–41.
- (3) R. Banerjee, A. Phan, B. Wang, C. Knobler, H. F.; M. O'Keeffe, O. Y. High-Throughput Synthesis of Zeolitic. *Science*. **2008**, *319*, 939–943.
- (4) Park, K. S.; Ni, Z.; Côté, A. P.; Choi, J. Y.; Huang, R.; Uribe-Romo, F. J.; Chae, H. K.; O'Keeffe, M.; Yaghi, O. M. Exceptional Chemical and Thermal Stability of Zeolitic Imidazolate Frameworks. *Proc. Natl. Acad. Sci. U. S. A.* **2006**, *103*, 10186–10191.
- (5) Tian, Y.-Q.; Yao, S.-Y.; Gu, D.; Cui, K.-H.; Guo, D.-W.; Zhang, G.; Chen, Z.-X.; Zhao, D.-Y. Cadmium Imidazolate Frameworks with Polymorphism, High Thermal Stability, and a Large Surface Area. *Chem. - A Eur. J.* **2010**, *16*, 1137–1141.
- (6) Hub, J. S.; De Groot, B. L.; Van Der Spoel, D. G_wham - a Free Weighted Histogram Analysis Implementation Including Robust Error and Autocorrelation Estimates. *J. Chem. Theory Comput.* **2010**, *6*, 3713–3720.
- (7) Verploegh, R. J.; Nair, S.; Sholl, D. S. Temperature and Loading-Dependent Diffusion of Light Hydrocarbons in ZIF-8 as Predicted Through Fully Flexible Molecular Simulations. *J. Am. Chem. Soc.* **2015**, *137*, 15760–15771.
- (8) Zhang, C.; Á, R. P. L.; Zhang, K.; Johnson, J. R.; Karvan, O.; Koros, W. J.; Biofuels, A.; Grande, B.; Springs, B.; States, U. Unexpected Molecular Sieving Properties of Z Eolitic Imidazolate F Ramewor K-8. **2012**, *8*–12.
- (9) Kwon, H. T.; Jeong, H. K.; Lee, A. S.; An, H. S.; Lee, J. S. Heteroepitaxially Grown Zeolitic Imidazolate Framework Membranes with Unprecedented Propylene/Propane Separation Performances. *J. Am. Chem. Soc.* **2015**, *137*, 12304–12311.